Cyclic Voltammetrically Prepared Copper-Decorated MnO$_2$ and its Electrocatalysis for Oxygen Reduction Reaction (ORR)

Ke-Qiang Ding

College of Chemistry and Materials Science, Hebei Normal University, Shijiazhuang 050016, P. R. China
[*]E-mail: dkeqiang@263.net

For the first time, copper particles were successfully prepared onto a MnO$_2$-modified graphite electrode by cyclic voltammetry (CV) technique, giving rise to a Cu-coated MnO$_2$-modified (denoted as Cu/MnO$_2$) graphite electrode. EIS(electrochemical impedance spectroscopy), SEM (scanning electron spectroscopy), EDS (electron diffraction spectroscopy) and FTIR (Fourier transform infrared spectrometry) were all employed to characterize the obtained samples, proving that Cu decorated MnO$_2$ composites were fabricated. And then, this resultant composite-modified graphite electrode was employed in oxygen reduction reaction (ORR) and the obtained cyclic voltammograms (CVs) strongly verified that ORR could proceed on this resultant composite. Lastly, the possible catalysis mechanism of Cu-MnO$_2$ towards ORR was proposed based on the results we acquired. Developing a novel substrate having Cu particles and MnO$_2$ on which ORR could proceed is the main contribution of this work.

1. INTRODUCTION

Recently, oxygen reduction reaction (ORR) has attracted many attentions due to its key applications in fuel cells [1, 2]. Although many kinds of fuel cells were developed so far, for example, proton exchange membrane fuel cell (PEMFC), direct methanol fuel cell (DMFC), direct ethanol fuel cell(DEFC), etc., oxygen reduction reaction(ORR) is the only employed cathodic reaction to receive electrons released from methanol, ethanol or other small organic molecules[3]. Consequently, all aspects concerning ORR, for example, the mechanism of ORR [4], the catalysts for ORR [5], are all under investigation. As reported, platinum is the main catalyst used for ORR, while, the sources of

platinum are limited and its cost is high, thus, non-platinum based catalysts are being widely explored [6].

Among the developed new catalysts for ORR, manganese oxides were also paid much more attentions now [7]. Actually, in 1973, it has been found by Zoltowski [8] that manganese oxides have catalysis towards oxygen reduction reaction (ORR), and in 1979, Brenet proposed that the catalysis of manganese oxides for ORR was due to the existence of Mn^{4+}/Mn^{3+} in manganese oxides [9]. Recently, Mao [10] et al. after investigating the catalysis of different kinds of manganese oxides on ORR, pointed out that γ–MnOOH exhibited the best catalysis for ORR among the employed manganese oxides, i.e., Mn_2O_3, Mn_3O_4 and Mn_5O_8. Very recently, Prof. Ohsaka [11] developed a gold nanoparticles-coated manganese oxide composite, and investigated its catalysis towards ORR. Nevertheless, due to lacking direct proofs, also owing to the complicated valence states of manganese oxides, till the present, unfortunately, the exact catalysis mechanism of manganese oxides for ORR was not achieved.

Because of its key applications in electronic industry, copper, especially its thin film, was widely investigated. Among various methods of copper thin film deposition onto substrates, such as PVD, CVD, and sputtering, the electrochemical methods (electroless and electrolytic) have proven to be least expensive, highly productive and readily adoptable [12]. To clarify the nucleation process of copper, also to extend the application of copper, copper has been electrodeposited onto various substrates. For instance, to probe the nucleation mechanisms of copper, near atomically smooth glassy carbon was used as the deposition substrate (electrode) by Grujicic [13]. Kelber [14] electrodeposited copper on Ru(001) in sulfuric acid solution with an intention to study the growth kinetics and nucleation behavior of copper. Pesic [15] discussed the reaction and nucleation mechanisms of copper electrodeposition from ammoniacal solutions on vitreous carbon. To the best of our knowledge, there is no paper reporting the electrodeposition of copper onto manganese oxides.

The application of copper in ORR has been well reported in terms of probing the corrosion behavior of copper rather than studying the application of ORR in fuel cells. For instance, Colley[16] studied ORR at copper microelectrodes in aqueous solution under conditions of high mass transport, proposing that the treatment of oxygen reduction as a 4-electron transfer process at micron and smaller-sized copper intermetallics in aluminium alloys may require revision. Jiang[17] investigated the kinetics of the oxygen reduction reaction on Cu(hkl) surfaces in perchloric acid and sulfuric acid solutions using rotating ring disk electrode, revealing that the mechanism of ORR is strongly influenced by the nature of the adsorbates. Lu [18] investigated the mechanisms of the cathodic ORR in a naturally aerated stagnant 0.5M H_2SO_4 using electrochemical methods, pointing out that in different potential regions various mechanisms of ORR were involved. While, to our knowledge, no paper reporting the catalysis of Cu-decorated manganese oxides towards ORR was published so far.

Herein, the composite of copper-decorated manganese oxides was prepared by a cyclic voltammetry (CV) method. SEM images, and EDS spectra as well, all strongly indicated that Cu-decorated MnO_2 (denoted as Cu/MnO_2) were successfully prepared onto on a graphite electrode in a Na_2SO_4 solution. More interestingly, results obtained from cyclic voltammograms (CVs) demonstrated that ORR could proceed on above Cu/MnO_2-modified electrode, and the catalysis mechanism of it

towards ORR was also discussed based on these results we obtained. Thus, a novel composite of Cu/MnO_2 was developed, which may be beneficial to explore novel catalyst for ORR.

2. EXPERIMENTAL PART

2.1. Chemicals

Manganese sulfate, sodium sulfate, copper sulfate and other reagents were all bought from Tianjin Chemical Reagent Co. Ltd (China). All other chemicals were used as received without further purification and all aqueous solutions were prepared using redistilled water. All used electrodes were purchased from Tianjin Aida Co., Ltd (China).

2.2. Electrodeposition of MnO_2 onto a graphite electrode

Electrodeposition was carried out on a CHI 660B electrochemical workstation (Shanghai Chenhua Apparatus, China) connected to a personal computer. A three-electrode configuration was employed, in which a graphite electrode (diameter is 3 mm) or a MnO_2-coated graphite electrode was used as the working electrode, and a platinum foil ($1cm^2$) as the counter electrode and saturated calomel electrode (SCE) as the reference electrode.

The preparation of MnO_2 onto a graphite electrode by cyclic voltammetry (CV) has been described in our previous paper [19]. Typically, in an aqueous solution of 0.5M H_2SO_4 containing 0.5 M $MnSO_4$, a well-treated graphite electrode was used as the working electrode, and a platinum foil ($1cm^2$) and saturated calomel electrode (SCE) were employed as the counter electrode and reference electrode, respectively. The applied potential range was from -0.2 V to 1.0V versus SCE, and the potential was scanned for 10 cycles at 50mV/s. After electrodeposition the MnO_2-coated graphite electrode was thoroughly rinsed by redistilled water and dried in ambient air. And then, the obtained MnO_2-coated graphite electrode was used as a working electrode in the electrodeposition of copper particles. The electrodeposition of copper was carried out in a 0.1 M solution of Na_2SO_4 having 0.01 M $CuSO_4$, in which the working electrode is the MnO_2-coated graphite electrode and the potential was cycled between -0.4V and 0.4V at a scan rate of 50mV/s for various cycles.

2.3. Characterization

Scanning electron microscopy (SEM) was performed on a Hitachi S-570 microscope (Japan) operated at 20kV. Electron dispersive X-ray analysis (EDS, PV-9900, USA) was analyzed by the WD-8X software established by Wuhan University of China. Fourier transform infrared spectrometry (FTIR) measurements were carried out on a Hitachi FTIR-8900 spectrometer (Japan). And electrochemical experiments were all conducted on a CHI 660B electrochemical workstation (Shanghai Chenhua Apparatus, China).
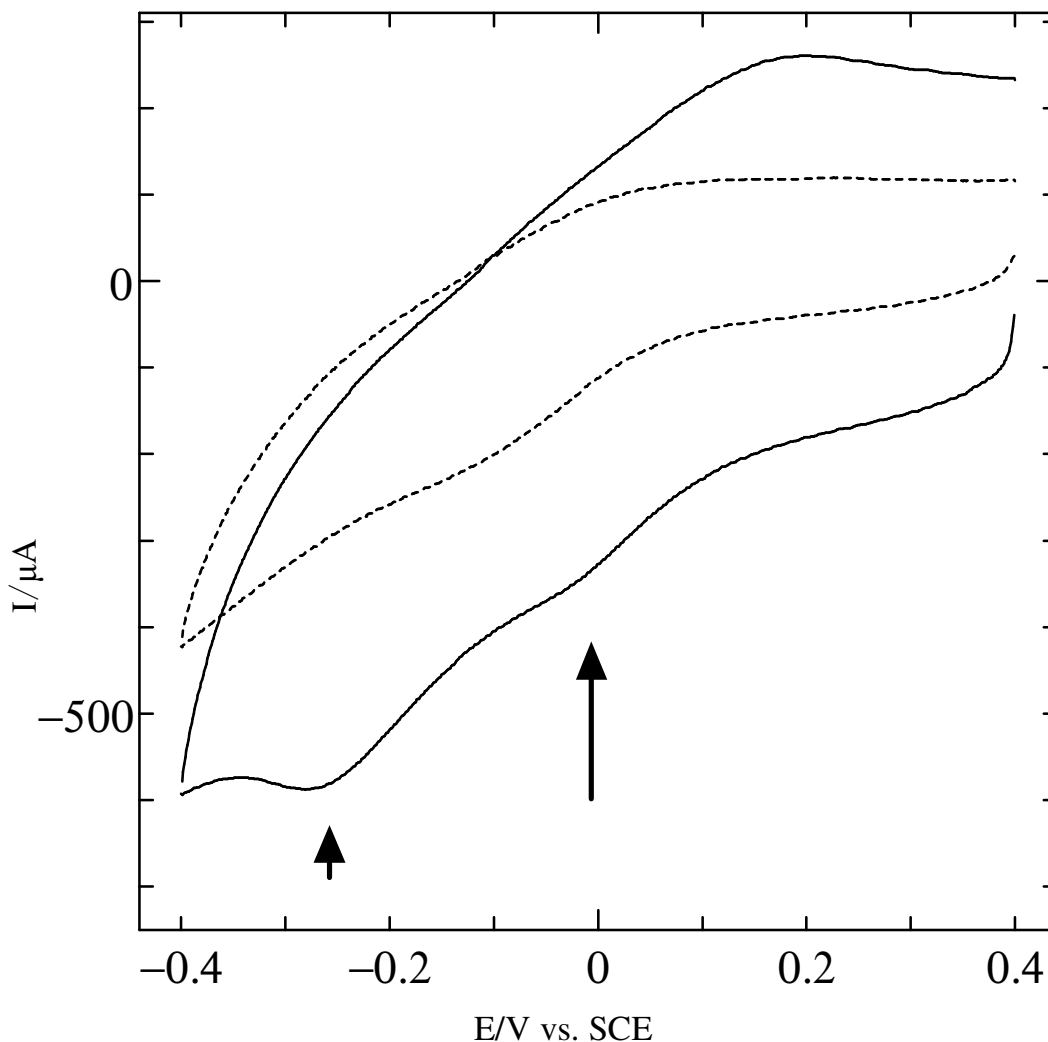
Figure 1. CVs obtained on a MnO_2-modified graphite electrode in 0.1M Na_2SO_4 solution. Dotted line : obtained in 0.1 M Na_2SO_4; solid line : in 0.1 M Na_2SO_4 containing 0.01M $CuSO_4$. Scan rate: 50mV/s.

3. RESULTS AND DISCUSSION

3.1. Electrodepostion of Cu particles onto MnO₂

Fig.1 displays the cyclic voltammograms (CVs) obtained on a MnO_2-modified graphite electrode, in which the dotted line was plotted in 0.1 M Na_2SO_4 and the solid line was measured in a 0.1 M Na_2SO_4 solution containing 0.01M $CuSO_4$. It can be seen that in the absence of $CuSO_4$, there is no evident peak appearing in the whole potential range. Interestingly, in the presence of $CuSO_4$, an evident reduction peak at -0.28V is clearly exhibited, suggesting that Cu^{2+} was reduced at this

potential. Another weak reduction peak close to 0V probably corresponds to the reduction reaction of $Cu^{2+} + e \rightarrow Cu^{+}$, as discussed in the previous report [15].
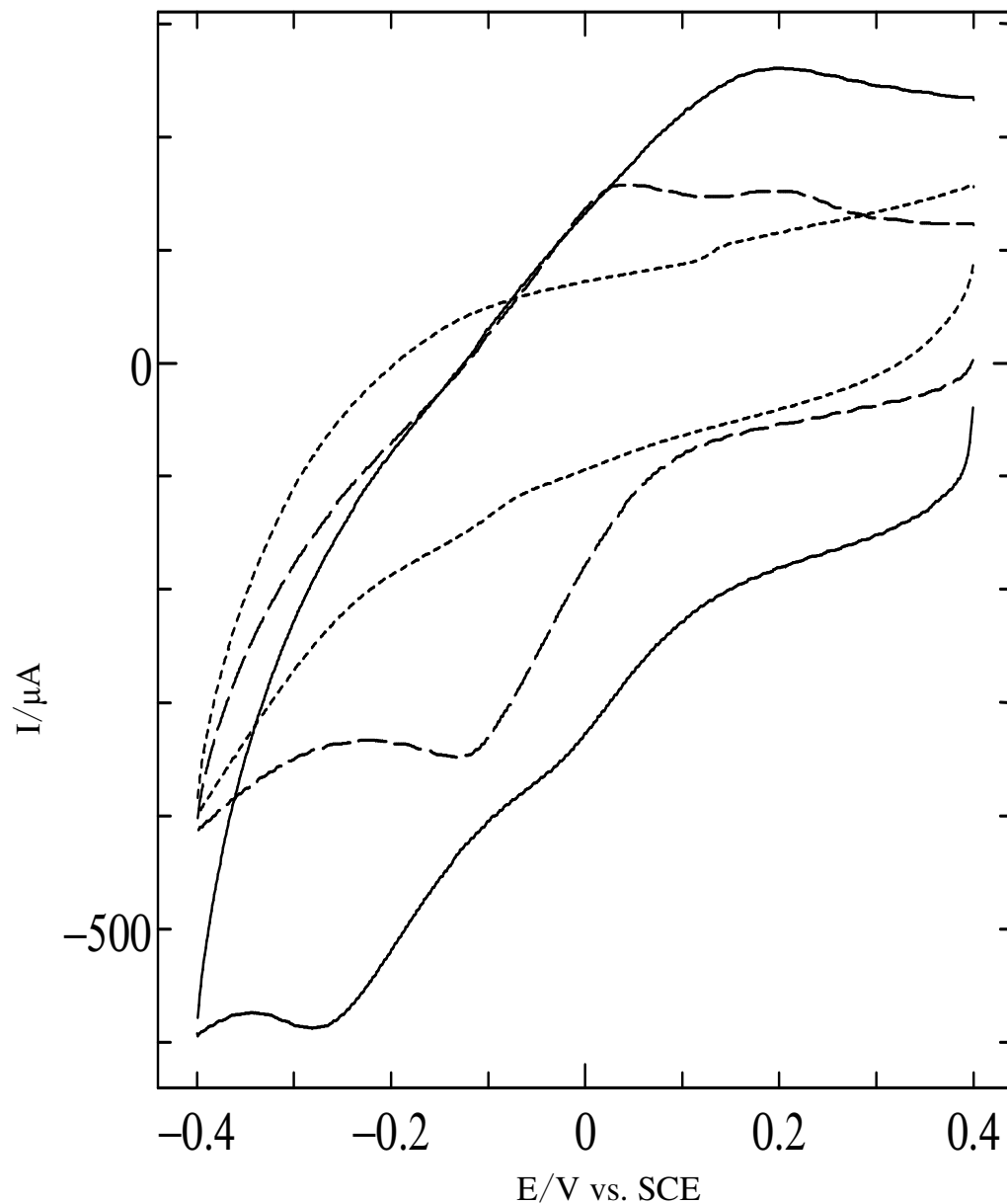
Figure 2. CVs in 0.1M Na_2SO_4 containing 0.01M $CuSO_4$ on various electrodes. Dashed line: on a graphite electrode; solid line: on a MnO_2-modified graphite electrode. Note: the dotted line was measured in 0.1M Na_2SO_4 on a graphite electrode. Scan rate: 50mV/s.

To clarify the peaks exhibited at around -0.28V, the CVs of Cu^{2+} on a bare graphite electrode was also recorded as shown in Fig.2. As shown by the dashed line, on the bare graphite electrode, an obvious reduction peak was observed, which can only be attributed to the reduction of Cu^{2+}. Also two weak oxidation peaks are exhibited in the positive-direction potential sweep, corresponding to two

electrochemical oxidation processes [15]. At the MnO_2-modified graphite electrode, as shown by the solid line in Fig.2, the shape of CVs corresponding to the electrochemical reduction of Cu^{2+} was greatly distorted. The reduction peak was divided as two successive reduction peaks as shown in Fig.1, meanwhile, two oxidation peaks, observed on the graphite electrode, emerged as one broad oxidation peak. This evident distortion of CVs strongly indicated that MnO_2 have participated in the electrochemical reaction of Cu^{2+}. Moreover, CVs of Cu^{2+}, exhibited on the MnO_2-modified graphite electrode, has a larger double-layer charge-discharge current compared to that on the bare graphite electrode, mainly because of the fact that MnO_2 is an ideal capacitance material [20].
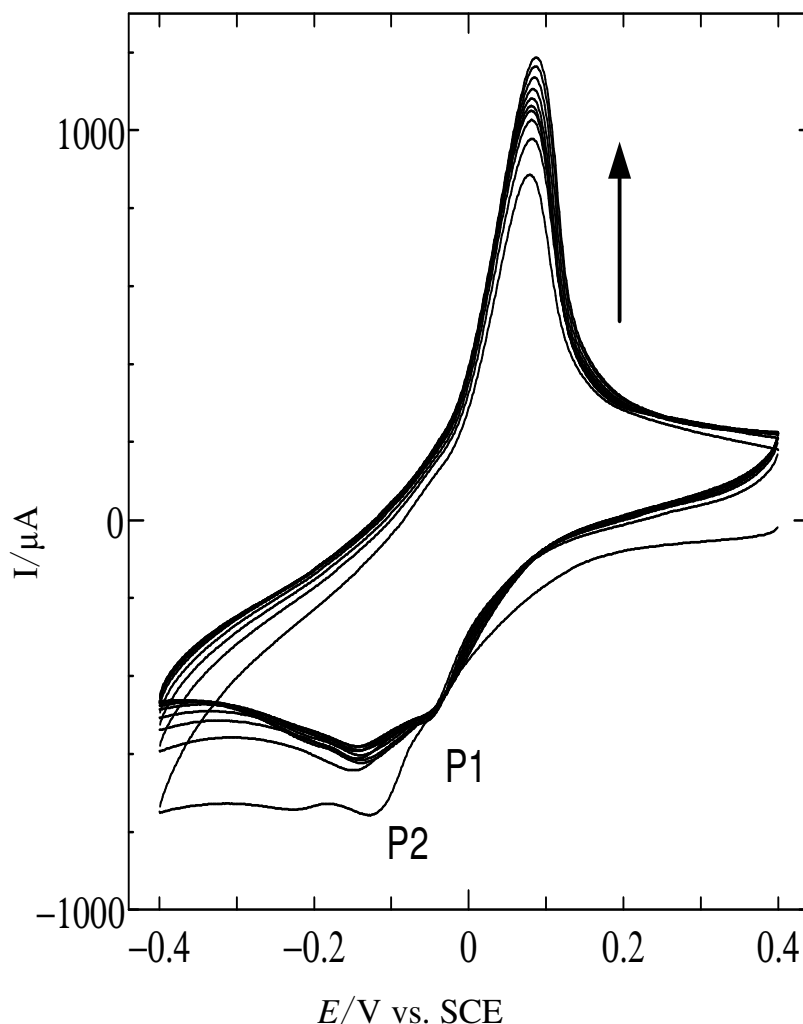
Figure 3. CVs obtained on a MnO_2-modified graphite electrode in 0.1M Na_2SO_4 containing 0.01M $CuSO_4$, in which the potential was scanned for 10cycles at 50mV/s

Fig.3 is the CVs obtained on a MnO_2-modified graphite electrode at the scan rate of 50mV/s for 10cycles in 0.01 M $CuSO_4$ solution. Interestingly, the peak current, especially for the anodic peaks, increased with the potential scan numbers, which are very similar to the previous investigation [15]

that was conducted on a vitreous carbon. As reported [15], the reduction peak labeled P1 is the electrochemical reaction (1), which was followed by a chemical reaction (2), generating copper atoms on the surface of MnO_2. The peak labeled P2 is the direct electrochemical reduction of Cu^{2+}, i.e., reaction (3), yielding copper atoms.

$$Cu(H_2O)_6{}^{2+} + e = Cu(H_2O)_4{}^+ \qquad (1)$$
$$2Cu(H_2O)_4{}^+ = Cu + Cu(H_2O)_6{}^{2+} \qquad (2)$$
$$Cu(H_2O)_6{}^{2+} + 2e = Cu + 6H_2O \qquad (3)$$
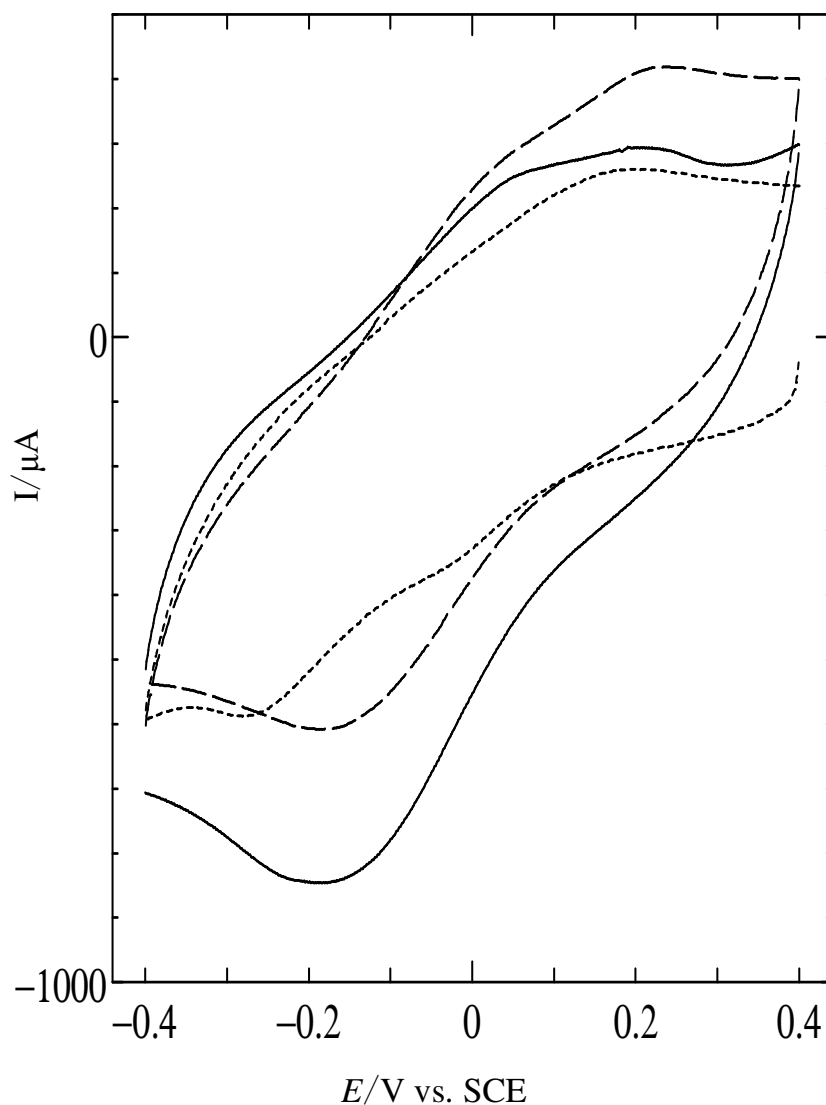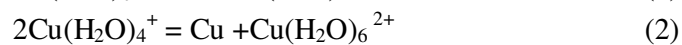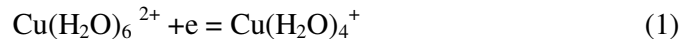
Figure 4. CVs obtained on a MnO_2-modified graphite electrode in 0.1M Na_2SO_4 having different concentrations of $CuSO_4$. Dotted line: in 0.01M $CuSO_4$; dashed line: in 0.015M $CuSO_4$; solid line: 0.02M $CuSO_4$. Scan rate: 20mV/s

To our surprise, the oxidation peak shown in Fig.3 is rather different from the previous report [15]. In our case, only one shaper oxidation peak is exhibited instead of two oxidation peaks. It was reported that the main oxidation peak displayed corresponds to the direct oxidation of Cu to generate $Cu(H_2O)_6^{2+}$, i.e., $Cu + 6H_2O \rightarrow Cu(H_2O)_6^{2+} +2e$[15], and another weak oxidation peak corresponds to the reaction, i.e., $Cu(H_2O)_4^{+}+ 2H_2O \rightarrow Cu(H_2O)_6^{2+}+ e$. Here, in our CV curves, the weak oxidation peak was not observed. Probably, in the presence of MnO_2, the produced $Cu(H_2O)_4^{+}$ was consumed by the reaction, i.e., $MnO_2 + Cu(H_2O)_4^{+}+ H_2O \rightarrow Cu(H_2O)_6^{2+} + MnOOH$ before $Cu(H_2O)_4^{+}$ was electrochemically oxidized to be $Cu(H_2O)_6^{2+}$, as a result, only one oxidation peak was presented. Additionally, with the increase of potential cycling number, the oxidation peak current was promoted evidently, as shown by the arrow, probably due to the fact that during the negative-potential sweep, more copper atoms were electrodeposited onto the surface of MnO_2, thus, in the positive-direction potential scanning, more copper atoms were electrochemically oxidized, leading to an augment of the oxidation peak current. Also, it can be inferred that some substance were formed on the surface of MnO_2 based on the fact that the oxidation peak currents increased with the potential cycling number.

To confirm the electrochemical reaction of Cu^{2+} on the surface of MnO_2, CVs of Cu^{2+} with different concentrations are shown in Fig.4. The dotted line was plotted in the solution of 0.01M $CuSO_4$, the dashed line and solid line are for the 0.015M, 0.02M $CuSO_4$ solution, respectively. One can see that with the increase of concentration, the reduction peak, and the oxidation peak as well, were all enhanced obviously, strongly supporting that the peaks we observed are stemmed from the electrochemical reaction of Cu^{2+}. Besides, the shapes of these CVs shown in Fig.4 are not regular, probably suggesting that the reaction of Cu^{2+}, including its chemical reaction and electrochemical reaction, on the surface of MnO_2 relates with the concentration of Cu^{2+} closely due to the presence of MnO_2. To the best of our knowledge, there is no paper reporting the electrochemical behavior of Cu^{2+} on the surface of MnO_2 though a heterobimetallic complexes having Cu and Mn has been synthesized recently in terms of its magnetic properties [21].

3.2. Characterization of the obtained Cu decorated -MnO₂

Electrochemical impedance spectroscopy (EIS), a powerful technique [22, 23] to describe the coated electrode, was used to characterize our obtained Cu/MnO_2 –modified graphite electrode. Nyquist plots, shown in Fig.5, were obtained at the open circuit potential over the frequency range from 0.1 to 10^5 Hz for the Cu/MnO_2-modified graphite electrode in 0.1 M Na_2SO_4, in which copper was electrodeposited by CV at 50mV/s for 10cycles in a $CuSO_4$ solution having various concentrations. For the MnO_2-modified graphite electrode, as shown by the squared line, there is a line (larger than 45°) in the whole frequency region, according with the previous report very well[24], also supporting that MnO_2 is a capacitance material. While, when Cu was electrodeposited on the surface of MnO_2, the Nyquist plots were substantially altered. For example, as illustrated by the rhombused curve, in which the concentration of $CuSO_4$ was 0.02M, the 45° line appearing in the lower frequencies region was totally suppressed, similar to the Nyquist plot of pure copper electrode very well[18], suggesting that Warbug diffusion process was greatly inhibited. Generally, MnO_2

prepared by CV has a porous structure [19], thus, owing to the formation of Cu particles on the surface of MnO_2, more pores were stuffed, therefore, the diffusion paths were blocked, leading to a nearly semicircle appearing in the whole frequency region, as illustrated by the rhombused curve in Fig.5. One can see that, with the increase of concentration of Cu^{2+}, there is an evident transition that occurred from a nearly pure capacitance element (larger than $45°$) to a diffusion character($45°$ line), and then to a parallel circuit (i.e., a semicircle). Generally speaking, the semicircle should be interpreted by a resistance element in parallel with a capacitor element [25]. For the pure MnO_2-modified electrode, someone proposed that the reaction, i.e., $MnO_2 + H^+ + e^- \rightarrow MnOOH$ [26], was involved, while other authors [27] proposed a modified reaction, i.e., $MnO_x(OH)_y + \delta H^+ + \delta e^- \rightarrow MnO_{x-\delta}(OH)_{y+\delta}$, to explain the capacitance behavior of MnO_2. Although the Nyquist plots of manganese oxides and that of copper electrode [18] have been well discussed, the exact interpretations were seldom reported so far. How do we explain the Nyquist plot for this obtained bimetallic material? More detailed investigations are really required.
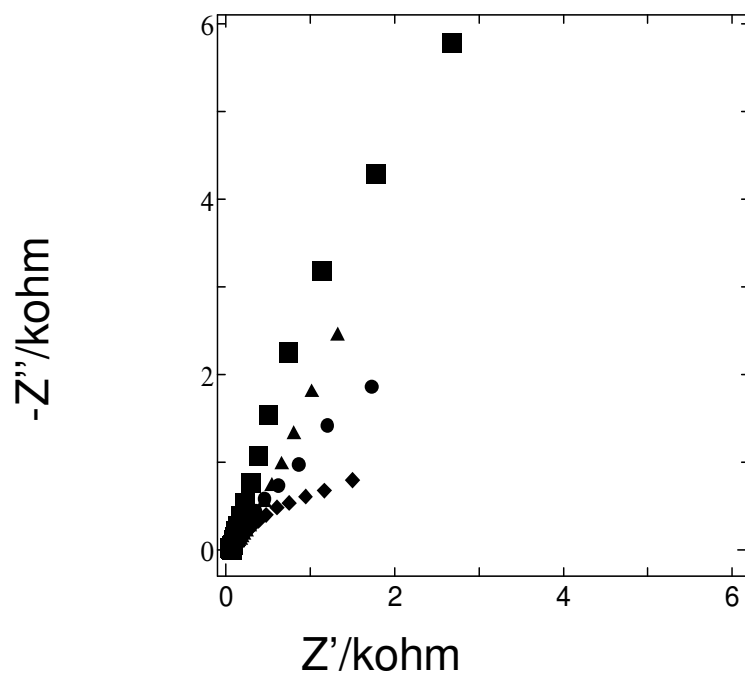
Figure 5. Nyquist plots obtained on a Cu/MnO_2-modified graphite electrode, in which Cu was electrodeposited in 0.1M Na_2SO_4 having various concentrations of $CuSO_4$ by CV for 10 cycles at 50 mV/s. squared line （■）: for a pure MnO_2-modified graphite electrode; triangled line （▲）: Cu was prepared in 0.01M $CuSO_4$, circled line （●）: Cu was prepared in 0.015M $CuSO_4$, rhombused line （♦）: Cu was prepared in 0.02M $CuSO_4$.

Fig.6 is the images for our obtained samples. It can be seen that particles of MnO_2 with irregular and loose structure are clearly exhibited by image A of Fig.6, very similar to the reported powder of MnO_2 [28]. It should be mentioned that the morphology of MnO_2 was substantially

dependent on the preparation conditions [19], such as, the potential scan rate, the potential scan range, and etc., which is out of the scope of this research work. Interestingly, as Cu was electrodeposited, more regular and bright particles are displayed, indicating that the pores of MnO_2 were fully stuffed by the formed Cu particles, consistent with the Nyquist plot of rhombus-lined curve shown in Fig.5 very well. The inset of image B is the EDS spectra for image B, in which the peaks corresponding to copper and manganese elements are all well exhibited, testifying that copper particles were really electrodeposited on the surface of MnO_2 by CV.
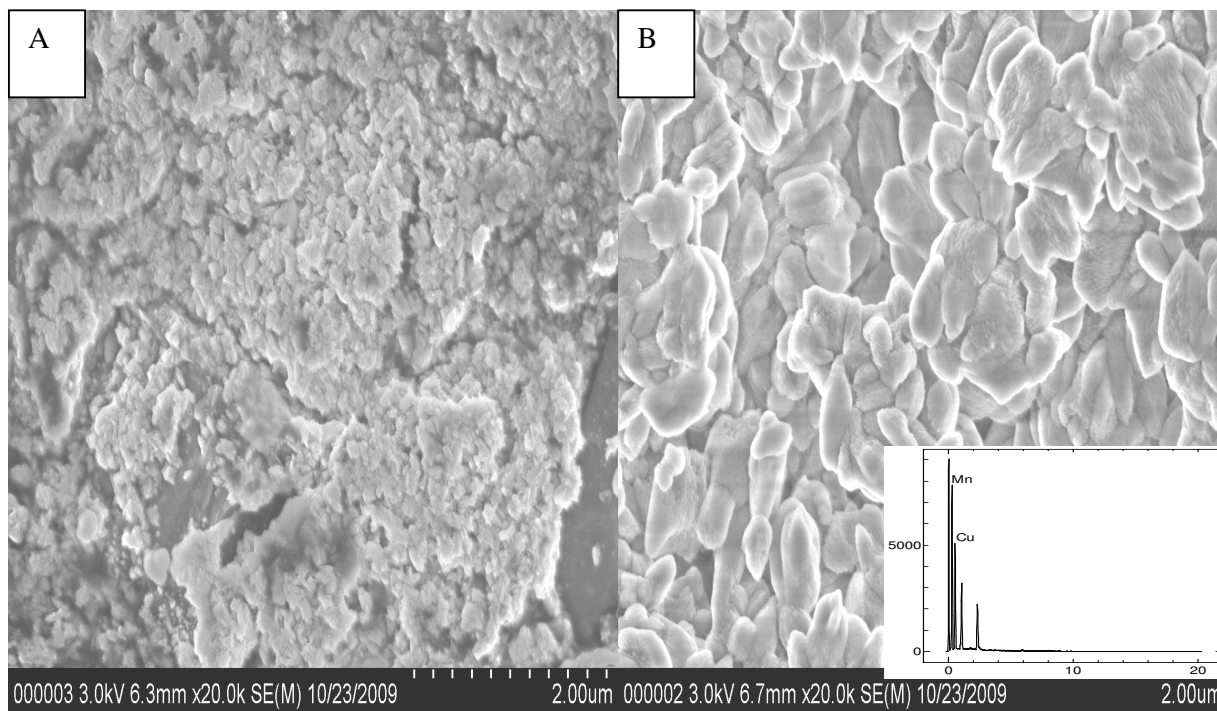
Figure 6. SEM images for the obtained samples. Image A: for MnO_2; Image B: Cu/MnO_2 composite. Inset in image B is the EDS spectra for the sample of image B.

Fig.7 is the FTIR spectra for the obtained samples. For the pure MnO_2, the presence of OH groups and H_2O as bound water in the mineral structure can be denoted by the peaks around $3415 cm^{-1}$ and $1618 cm^{-1}$[29]. And peaks appearing in the range $500–800 cm^{-1}$ were considered as characteristics of $\gamma-MnO_2$ [29], thus based on FTIR spectra, it was confirmed that manganese oxides we prepared are mainly MnO_2 rather than other kinds of manganese oxides. While, for the Cu/MnO_2 sample, no other peaks were observed except for the peak at $1070 cm^{-1}$ as illustrated by empty circle, suggesting that the resultant Cu particles have no strong influence on the structure of MnO_2. As reported previously [30], the absorption peak at $1117 \ cm^{-1}$ was resulted from the interaction of Mn with surrounding species such as OH and O atoms or groups, thus, probably, the introduction of Cu affected the interaction between Mn and OH or O. As a result, a novel peak at $1070 cm^{-1}$ was displayed. Or, probably, some

formed Cu atoms interacted with O atom to yield Cu-O-Mn like bonds [30] leading to an appearance of novel peak at around 1070cm^{-1}. Here, FTIR spectra not only proved the formation of MnO_2 on the graphite electrode, but also indicated that there is an interaction between MnO_2 and formed Cu atoms, though the essence of this interaction was not very clear at present stage.
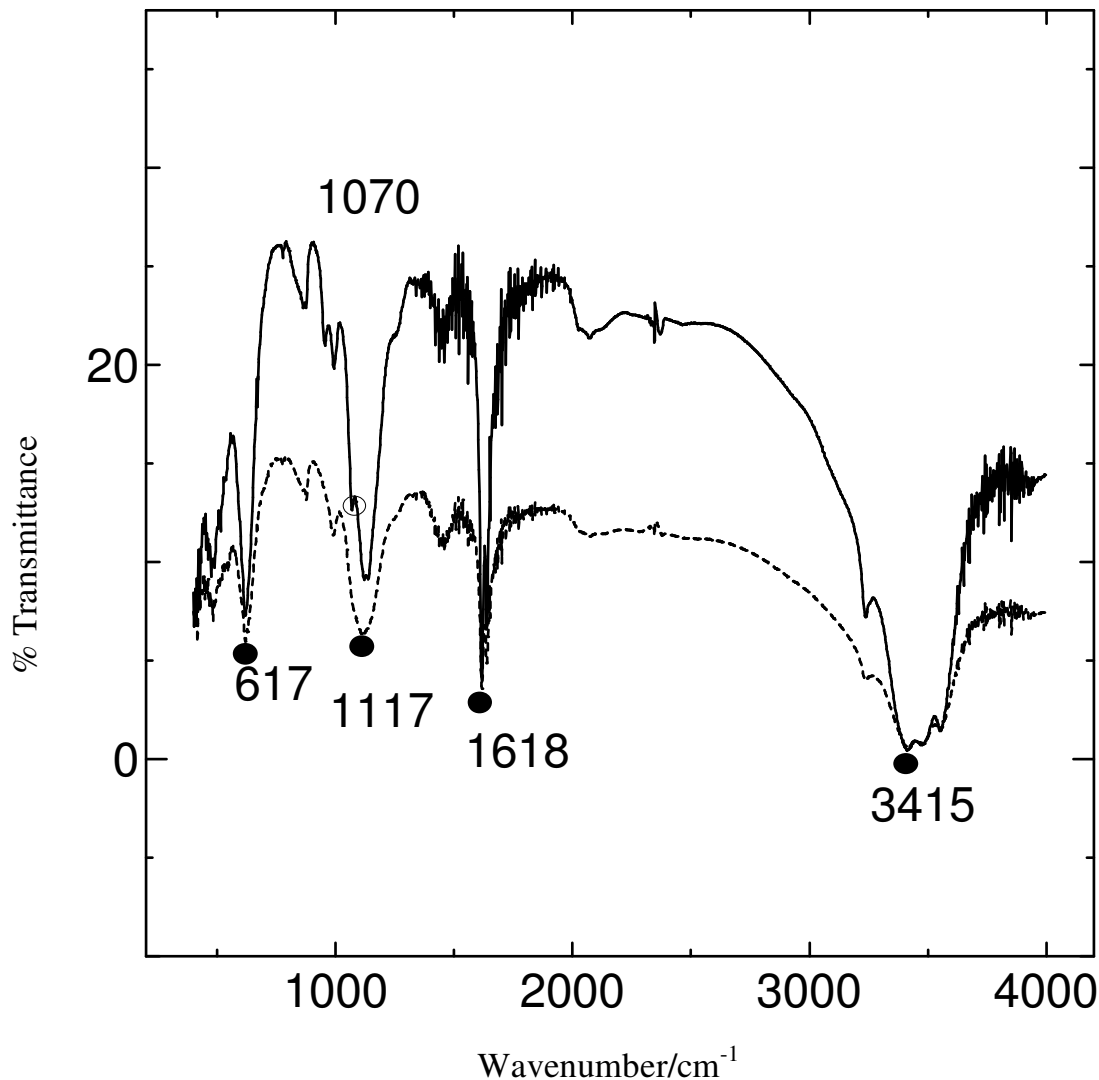
Figure 7. FTIR spectra for the obtained samples. Dotted line: for MnO_2; solid line: Cu/MnO_2 composite.

3.3. Electrocatalysis of Cu/MnO$_2$ composite towards oxygen reduction reaction (ORR)

Developing non-platinum based catalysts for ORR is a main research work due to the limited resource of Pt and its high cost. Hence, developing Pt-free substrates on which ORR could proceed was paid much more attention. Here, we utilized this novel composite of Cu/MnO_2 towards ORR for the first time.
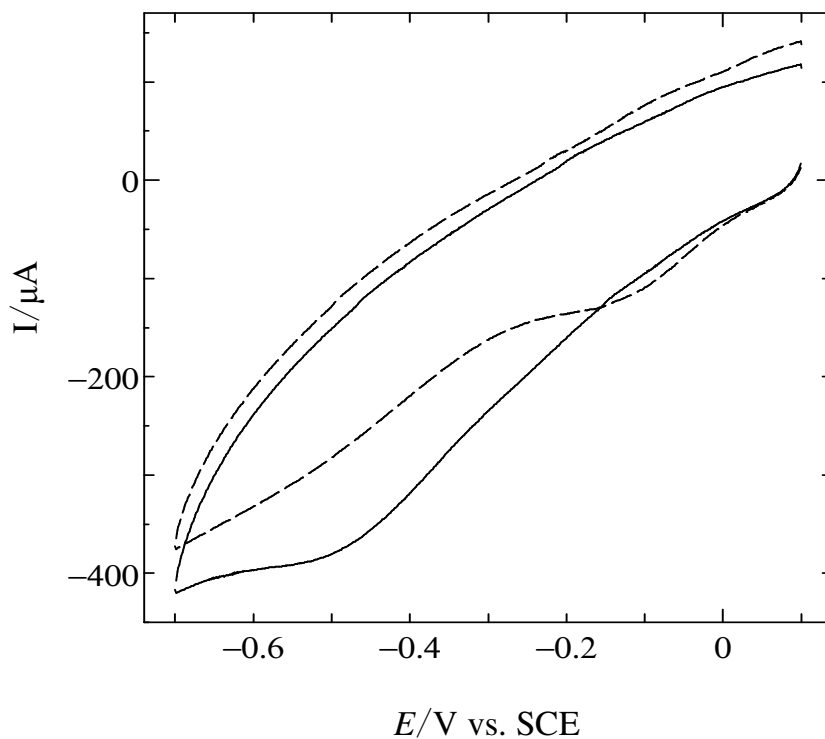
Figure 8. CVs obtained on a Cu/MnO$_2$ modified graphite electrode in 0.1M Na$_2$SO$_4$ solution. Dashed line: obtained in a nitrogen saturated 0.1M Na$_2$SO$_4$ solution; solid line: in an oxygen –saturated 0.1M Na$_2$SO$_4$ solution. Scan rate: 20mV/s.

Fig.8 presents the CVs obtained on a Cu/MnO$_2$ modified graphite electrode. As shown by the dashed line, in the nitrogen gas saturated solution, no evident reduction peak was found in the employed potential range, though a small reduction peak was observed at around -0.1V probably corresponding to the reduction reaction of MnO$_2$, MnO$_2$+e$^-$ +H$^+$→MnOOH [26]. While, in the oxygen-saturated 0.1M Na$_2$SO$_4$ solution, an evident reduction peak was observed at about -0.5V. Thus, one can confirm that the reduction peak at -0.5V is attributed to the electrochemical reduction of oxygen molecules. The influence of scan rate on the CVs of ORR was also carried out as shown in Fig.9, in which well-defined CVs were displayed, very similar to the CVs of ORR on carbon nanofibers (CNF)[31]. Also, a linear relationship between the reduction peak currents and the square root of scan rates was gained (data not shown here), strongly verifying that ORR is a diffusion-controlled process on this novel composite of Cu-MnO$_2$. Fig. 8 and Fig.9 strongly demonstrated that ORR could proceed on this novel composite of Cu/MnO$_2$.

To probe the stability of this novel composite of Cu/MnO$_2$, the used Cu/MnO$_2$ modified graphite electrode was conserved in a refrigeratory for a week. And then it was used to detect CVs of ORR once again. Interestingly, CVs of ORR can also be clearly exhibited, as presented in Fig.10, suggesting that it is feasible to apply this novel electrode in ORR occurring in fuel cells.

We must admit that ORR on MnO$_2$ (or MnOx) has been investigated by many researching groups. However, the exact interpretation of its catalysis towards ORR was not achieved. For instance,

Xu [7] prepared manganese oxides and probed its catalysis for ORR in alkaline solution, proposed that high composition freedom and higher corrosion resistance of MnO_2 might be responsible for its catalysis for ORR. Professor Ohsaka [32] thought that O_2 reduction at the MnOOH-modified glassy carbon (GC) electrodes undergoes an electrochemical process followed by sequent disproportions of the electrochemical reduction intermediates, i.e., superoxide anion (O_2^-) and hydrogen peroxide (HO_2^-). As for the mechanism of ORR on copper electrode, there are also several propositions, as addressed in ref. [18] and ref. [16]. Thus, to a conclusion, the mechanism of ORR still remains unresolved.
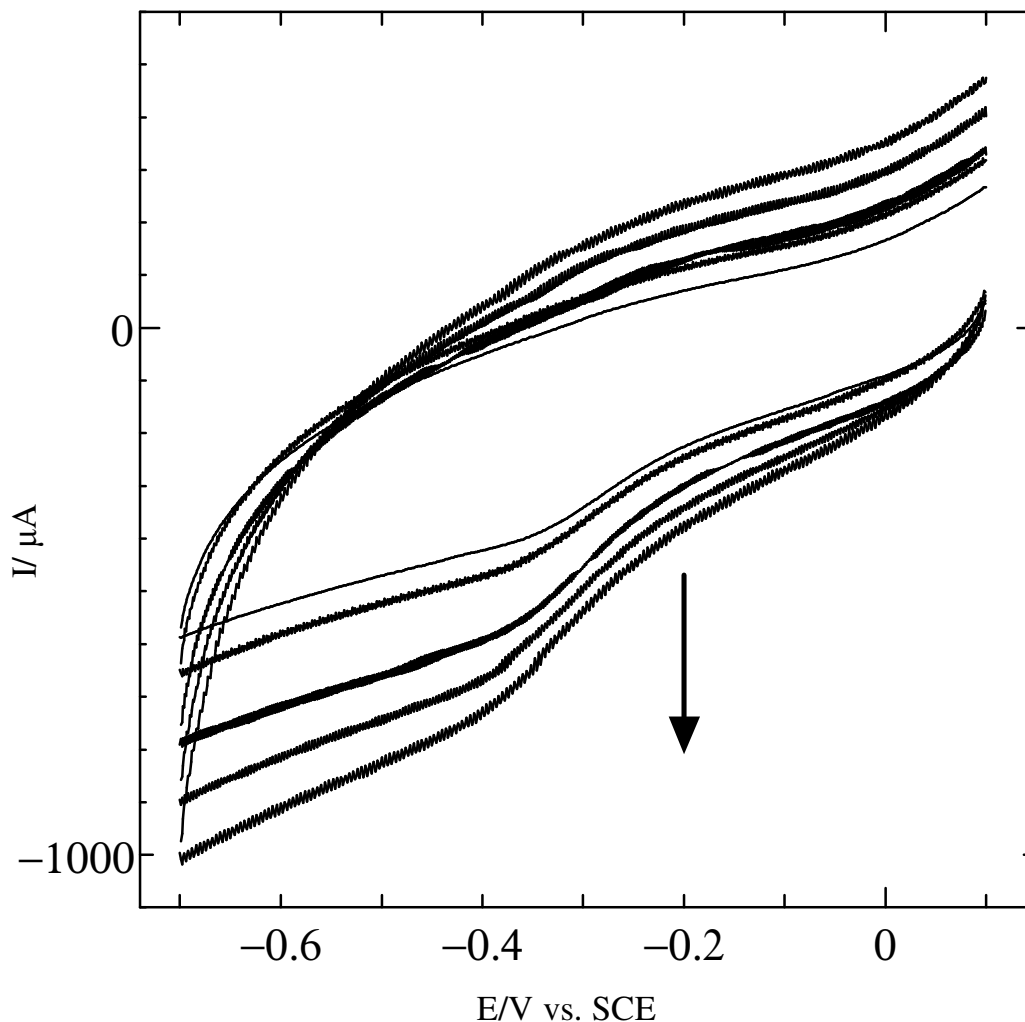
Figure 9. CVs of ORR on a Cu/MnO_2 modified graphite electrode in an oxygen–saturated aqueous 0.1M Na_2SO_4 solution. Scan rate: 50, 80,100,150 and 200mV/s.

Since oxygen molecule has a strong tendency to adsorb on the surface of copper [18], thus, probably, the following process occurred on our developed substrate of $Cu-MnO_2$.

$$(O_2)_{sol} + Cu \rightarrow (Cu)\text{-}(O_2)_{ads} \qquad (1)$$

$$MnO_2 + e + H_2O \rightarrow MnOOH \qquad (2) \text{ or}$$

$$MnO_2 + Cu(H_2O)_4^+ + H_2O \rightarrow Cu(H_2O)_6^{2+} + MnOOH \qquad (3)$$

$$(Cu)\text{-}(O_2)_{ads} + MnOOH \rightarrow Cu + O_2^- + MnO_2 \qquad (4)$$

$$O_2^- + H^+ \rightarrow H_2O_2 \text{ or } H_2O \qquad (5)$$
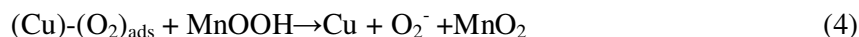
That is to say, firstly, the dissolved oxygen molecules in solution were adsorbed on the surface of copper spontaneously, and meanwhile, in the negative potential region, MnO_2 accepts one electron to generate molecules of MnOOH, or MnO_2 reacts with the formed $Cu(H_2O)_4^+$ to yield MnOOH. Subsequently, MnOOH was oxidized by the adsorbed oxygen molecules to form MnO_2 again. Part of the formed superoxide anion reacted with protons to yield H_2O_2 or H_2O directly.
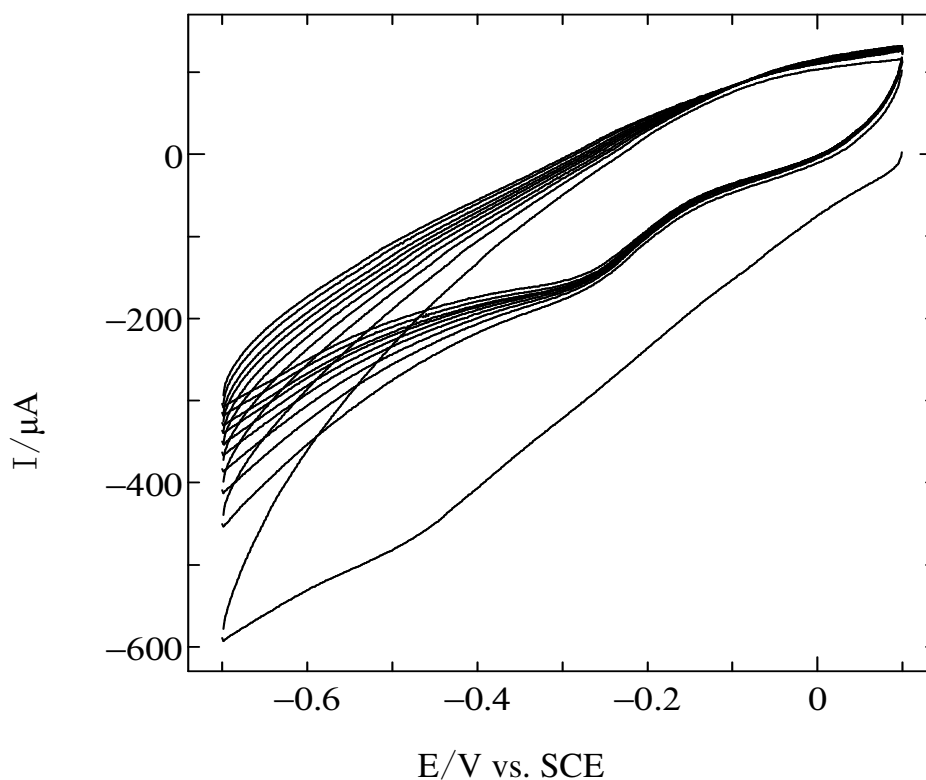
Figure 10. CVs of ORR on a Cu/MnO_2 modified graphite electrode in an oxygen saturated 0. 1M Na_2SO_4 solution at 20mV/s for 10cycles.

The path proposed here is only a speculated mechanism, and more direct proofs are really needed to present a satisfied interpretation on the mechanism of ORR on this novel substrate of Cu/MnO_2. Also, there are many questions suspended, for instance, what is the interaction between copper particles and MnO_2? How does the mass ratio of MnO_2 to Cu affect the process of ORR? And so on. Further works are under consideration in our lab.

4. CONCLUSIONS

For the first time, a composite of Cu decorated MnO_2 was prepared by CV method from an aqueous solution of Na_2SO_4 having $CuSO_4$, and the obtained samples were characterized by EIS, SEM and FTIR, respectively. The obtained results indicated that copper particles were really generated onto MnO_2, giving rise to a novel composite of Cu-decorated MnO_2. More importantly, this novel composite was employed for oxygen reduction reaction (ORR) for the first time, and the obtained CVs strongly testified that ORR could proceed on the Cu/MnO_2 modified graphite electrode. Lastly, the possible catalysis mechanism of this Cu/MnO_2 composite towards ORR was proposed based on our data and previous reports. We do admit that due to the complicated valence state of manganese oxide, the exact interpretation of this composite having copper and MnO_2 for ORR is still suspended, and more investigations are really needed.

References

1. Y. Tang, B. L. Allen, D. R. Kauffman, A. Star, *J. Am. Chem. Soc.* 131 (2009) 13200.
2. Z. Peng, H. Yang, *J. Am. Chem. Soc.* 131 (2009) 7542.
3. H. Meng, P. K. Shen, *Electrochem. Commun.* 8 (2006) 588.
4. T. Zhang, A. B. Anderson, *Electrochim. Acta* 53 (2007) 982.
5. P. Wang, Z. Ma, Z. Zhao, L. Jia, *J. Electroanal. Chem.* 611 (2007) 87.
6. M.-H. Shao, K. Sasaki, R. R. Adzic, *J. Am. Chem. Soc.* 128 (2006) 3526.
7. J. Yang, J. J. Xu, *Electrochem. Commun.* 5 (2003) 306.
8. P. Zoltowski, D.M. Drazic, L. Vorkapic, *J. Appl. Electrochem.* 3 (1973) 271.
9. J.P. Brenet, *J. Power Sources* 4 (1979) 183.
10. L. Mao, D. Zhang, T. Sotomura, K. Nakatsu, N. Koshiba, T. Ohsaka, *Electrochim. Acta* 48(2003) 1015.
11. M. S. El-Deab, T. Ohsaka, *Electrochim. Acta* 52 (2007) 2166.
12. G. Oskam, P.M. Vereecken, P.C. Searson, *J. Electrochem. Soc.* 146 (1999) 1436.
13. D. Grujicic, B. Pesic, *Electrochim. Acta* 47 (2002) 2901.
14. J. Kelber, S. Rudenja, C. Bjelkevig, *Electrochim. Acta* 51 (2006) 3086.
15. D. Grujicic, B. Pesic, *Electrochim. Acta* 50 (2005) 4426.
16. A. L. Colley, J. V. Macpherson, P. R. Unwin, *Electrochem. Commun.* 10 (2008) 1334.
17. T. Jiang, G.M. Brisard, *Electrochim. Acta* 52 (2007) 4487.
18. Y. Lu , H. Xu, J. Wang , X. Kong, *Electrochim. Acta* 54 (2009) 3972.
19. K.Q. Ding, *J. Chin. Chem. Soc.* 55 (2008) 543.
20. A. Zolfaghari, F. Ataherian, M. Ghaemi, A. Gholami, *Electrochim. Acta* 52 (2007) 2806.
21. A. O. Beznischenko , V. G. Makhankova , V. N. Kokozay , V. V. Dyakonenko, R. I. Zubatyuk , O. V. Shishkin , J. Jezierska, *Inorg. Chim. Acta* 362 (2009) 1307.
22. K.Q. Ding, Q. Wang, Z. Jia, R. Tong, X. Wang, H. Shao, *J. Chin. Chem. Soc.* 50 (2003) 387.
23. J. Gamby, P. L. Taberna, P. Simon, J. F. Fauvarque, M. Chesneau, *J. Power Sources* 101 (2001) 109.

24. S.-E. Chun, S.-I. Pyun, G.-J. Lee, *Electrochim. Acta* 51 (2006) 6479.
25. A. Manivel, N. Ilayaraja, D. Velayutham, M. Noel, *Electrochim. Acta* 52 (2007) 7841.
26. S. Nijjer, J. Thonstad , G.M. Haarberg, *Electrochim. Acta* 46 (2000) 395.
27. C.-C. Hu, T.-W. Tsou, *Electrochem. Commun.* 4 (2002) 105.
28. S.R. Sivakkumar , J. M. Ko, D. Y. Kim, B.C. Kim , G.G. Wallace, *Electrochim. Acta* 52 (2007) 7377.
29. F. Pagnanelli, C. Sambenedetto, G. Furlani, F. Vegliò, L. Toro, *J. Power Sources* 166 (2007) 567.
30. D. Visinescu , J.-P. Sutter , C. Ruiz-Pérez, M. Andruh, *Inorg. Chim. Acta* 359 (2006) 433.
31. J.-S. Zheng, X.-S. Zhang, P. Li , X.-G. Zhou, D. Chen,Y. Liu, W.-K. Yuan, *Electrochim. Acta* 53 (2008) 3587.
32. T. Ohsaka, L. Mao , K. Arihara , T. Sotomura, *Electrochem. Commun.* 6 (2004) 273.